Calcium channel and glutamate receptor activities regulate actin organization in salamander retinal neurons

Massimiliano Cristofanilli and Abram Akopian

Department of Ophthalmology, New York University School of Medicine, New York, NY 10016, USA

Intracellular Ca^{2+} regulates a variety of neuronal functions, including neurotransmitter release, protein phosphorylation, gene expression and synaptic plasticity. In a variety of cell types, including neurons, Ca^{2+} is involved in actin reorganization, resulting in either actin polymerization or depolymerization. Very little, however, is known about the relationship between Ca^{2+} and the actin cytoskeleton organization in retinal neurons. We studied the effect of high-K^+-induced depolarization on F-actin organization in salamander retina and found that Ca^{2+} influx through voltage-gated L-type channels causes F-actin disruption, as assessed by $53 \pm 5\%$ ($n = 23$, $P < 0.001$) reduction in the intensity of staining with Alexa-Fluor488-phalloidin, a compound that permits visualization and quantification of polymerized actin. Calcium-induced F-actin depolymerization was attenuated in the presence of protein kinase C antagonists, chelerythrine or *bis*-indolylmaleimide hydrochloride (GF 109203X). In addition, phorbol 12-myristate 13-acetate (PMA), but not 4α-PMA, mimicked the effect of Ca^{2+} influx on F-actin. Activation of ionotropic AMPA and NMDA glutamate receptors also caused a reduction in F-actin. No effect on F-actin was exerted by caffeine or thapsigargin, agents that stimulate Ca^{2+} release from internal stores. In whole-cell recording from a slice preparation, light-evoked 'off' but not 'on' EPSCs in 'on–off' ganglion cells were reduced by $60 \pm 8\%$ ($n = 8$, $P < 0.01$) by cytochalasin D. These data suggest that elevation of intracellular Ca^{2+} during excitatory synaptic activity initiates a cascade for activity-dependent actin remodelling, which in turn may serve as a feedback mechanism to attenuate excitotoxic Ca^{2+} accumulation induced by synaptic depolarization.

The important roles of intracellular Ca^{2+} and of Ca^{2+}-activated neuroregulatory processes in modulating ligand- and voltage-activated channels in retinal neurons have been extensively studied in recent years (reviewed by Akopian & Witkovsky, 2002). One of the major sources for intracellular Ca^{2+} elevation is calcium influx through voltage-activated Ca^{2+} channels, which are activated when cells receive excitatory drive through synaptic channels. Such changes in intracellular Ca^{2+} during synaptic transmission are associated with important physiological processes, such as synaptic plasticity, neuronal differentiation and neuromodulation (Chittajallu *et al.* 1998). Calcium is also implicated in neurodegeneration and cell death in such diseases as glaucoma and retinal ischaemia, in which neurotoxicity is caused by an excessive stimulation of glutamate receptors (reviewed by Sucher *et al.* 1997).

In a variety of cell types, one important action of Ca^{2+} influx is its ability to interfere with the structure of the actin cytoskeleton. The cytoskeleton is intimately involved in the regulation of cell motility, excitotoxicity, receptor activity and synaptic function (Neely & Gesemann, 1994; Furukawa *et al.* 1995; Oertner & Matus, 2005). Studies indicate that Ca^{2+} induces diverse changes in F-actin structure that in some cases appear contradictory. For instance, Ca^{2+} influx has been associated with increases in the F-actin network in goldfish retinal bipolar cell terminals (Job & Lagnado, 1998) and in the induction of filopodia in grasshopper neurons (Lau *et al.* 1999), whereas in hippocampal neurons, Ca^{2+} influx caused a depolymerization of F-actin and a dislocation of dendritic spines (Rosenmund & Westbrook, 1993; Furukawa *et al.* 1995; Halpain *et al.* 1998; Brunig *et al.* 2004). The reason for these apparent discrepancies is not clear. It is possible

that the different effects of Ca^{2+} on the actin cytoskeleton are associated with the presence of diverse Ca^{2+}-activated proteins, such as gelsolin and profilin, and their targeted substrates that produced differential actions on the actin cytoskeleton (Oertner & Matus, 2005).

In salamander retinal ganglion cells, actin depolymerization causes a reduction in Ca^{2+} influx through voltage-activated L-type channels (Schubert & Akopian, 2004) and glutamate receptor-activated channels (Akopian *et al.* 2006), but whether Ca^{2+} entry affected F-actin organization in third-order retinal neurons was unknown. In this study, we show that Ca^{2+} influx through high-voltage-activated L-type channels causes F-actin depolymerization in salamander retinal neurons by a protein kinase C (PKC)-mediated mechanism.

Methods

Tissue and cell preparation

The handling and maintenance of animals met the National Institute of Health guidelines and were approved by the Institutional Care and Use Committee at NYU School of Medicine. Salamanders (*Ambystoma tigrinum*) were anaesthetized in a bath of tricaine methanosulphonate ($100\ mg\ ml^{-1}$) until the animal no longer reacted to tactile stimulation, after which they were decapitated and double pithed. The eyes were cut in half; both retinas were removed and placed in control Ringer solution containing (mM): NaCl, 100; KCl, 3; $CaCl_2$, 2; $MgCl_2$, 2; and Hepes, 10; adjusted to pH 7.6 with NaOH. Eyecups were used for preparation of cryostat sections. To dissociate cells, retinas were incubated for 1 h at room temperature with oxygenated Ringer solution containing $14\ i.u.\ ml^{-1}$ of papain (Worthington Biochemicals, Lakewood, NJ, USA), $0.5\ mM\ Ca^{2+}$ per $25\ mM\ NaHCO_3$, 6 mg cysteine, 1 mM sodium pyruvate and 16 mM D-glucose. After rinses, retinas were dissociated in DMEM medium (Gibco, Carlsbad, CA, USA) using a wide-bore 5 ml pipette. The resulting cell suspension was plated on poly L-lysine-coated coverslips, and the cells were allowed to settle for 30–45 min before treatments.

Materials

Compounds were obtained from the following sources: Alexa-Fluor488-phalloidin (Molecular Probes, Eugene, OR, USA), glutamate, amino-3-hydroxy-5-methyl-4-isoxazolepropionic acid (AMPA), *N*-methyl-D-aspartate (NMDA), chelerythrine chloride, *bis*-indolylmaleimide hydrochloride (GF 109203X), ω-conotoxin GVIA, nifedipine, thapsigargin, phorbol 12-myristate 13-acetate (PMA) and 4α-PMA (all from Sigma, St Louis, MO, USA), latrunculin A and cytochalasin D (Biomol International, Plymouth Meeting, PA, USA).

F-Actin staining of retinal cryostat sections

Control and high-K^+-treated eyecups were fixed for 30 min in an ice-cold solution of 4% paraformaldehyde inphosphate-buffered saline (PBS; pH 7.4). After a wash, eyecups were dehydrated with 30% sucrose (overnight at 4°C), embedded in Tissue-Tek and sectioned at $15\ \mu m$ on a cryostat. To visualize actin filaments, sections were treated with 0.3% Triton X-100 for 5 min, pre-incubated for 30 min with 3% bovine serum albumin (BSA; with 0.1% Triton X-100 in PBS), and incubated for 2 h at room temperature (RT) with Alexa-Fluor488-phalloidin diluted in the BSA–Triton X-100 solution to a final phalloidin concentration of 0.2–$0.3\ \mu M$. After extensive rinsing, the tissues were mounted with Vectashield (Vector, Burlingame, CA, USA) and observed with a confocal laser-scanning microscope (Nikon Eclipse C-1; Nikon, Japan). Single-plane fluorescence images were acquired using the $\times 60$ or $\times 100$ oil-immersion objective lens and EZ-C1 software (Nikon). Images from control and high-K^+-treated samples were obtained with the same scanning parameters and were processed using Adobe Photoshop version 7.0 (Adobe Systems Inc., San Jose, CA, USA). To control for day-to-day variations in staining intensity, treated specimens were always compared with controls prepared the same day under identical fixation, permeabilization, staining and microscopy conditions, thus allowing meaningful comparisons among samples.

F-Actin staining of acutely dissociated retinal cells

Isolated cells treated with either control or drug-containing solutions were fixed for 30 min in an ice-cold solution of 4% paraformaldehyde, 4% sucrose in PBS (pH 7.4). To stain actin filaments with Alexa-Fluor488-phalloidin, we used the procedure described above. Coverslips were mounted with Prolong Antifade Mounting Medium (Molecular Probes) and observed with a confocal laser-scanning microscope. Viability of cells included in quantitative analysis was assessed by morphological criteria; only cells with intact processes (presumed amacrine or ganglion) and soma with a smooth appearance were considered. For each treatment, three to five independent experiments were carried out with 12 coverslips in each experiment, and at least 20 cells in each of the control and treated samples were monitored for phalloidin staining. To quantify the changes in the actin network, scans of pixel intensity were performed by linescan using Metavue software (Universal Imaging Co., Downington, PA, USA) and the intensity profile was obtained along a line drawn through the centre of the dissociated cells, or by means of a bar ranging from the outer limit of the outer plexiform layer (OPL) to the inner limit of the inner plexiform layer (IPL) in vertical

sections. For statistical analysis, the intensity at two peaks representing F-actin at either side of the cell was measured under different experimental conditions and normalized to a control value for a given series of experiments. All pooled data are presented as $n \pm$ S.E.M. with n indicating the number of neurons tested. Levels of significance were assessed using Student's paired t test. Fluorescence intensities are indicated in arbitrary units (a.u.) from 0 to 250. A P value of less than 0.05 was considered to indicate statistical significance in all of the analysis.

Electrophysiology

Under dim red light illumination, retinas were isolated from the eyecup and placed over a piece of Milli-pore filter paper (pore size, 0.45 μm), with the ganglion cell layer facing up, and were cut into 150–200 μm slices with a custom-made slicer. Whole-cell patch clamp recordings were made from 'on–off' ganglion cells in the slice preparation using ~5 MΩ electrodes containing (mM): potassium gluconate, 100; MgCl$_2$, 2; CaCl$_2$, 0.2; EGTA, 2; Hepes, 10; ATP, 2; and GTP, 0.1; adjusted to pH 7.3 with KOH. The bath (Ringer) solution contained (mM): NaCl, 100; KCl, 3; CaCl$_2$, 2; MgCl$_2$, 2; and Hepes, 10; adjusted to pH 7.6 with NaOH. Strychnine (20 μM) and picrotoxin (80 μM) were added to the bath solution to block glycinergic and GABAergic trans-missions, respectively. The voltage- and current-clamp recordings were made with an Axopatch 200B amplifier. Analog signals were filtered at 1 kHz and sampled at 2 kHz with the Digidata 1322A analog-to-digital board. The PClamp8 software package (Axon Instruments) was used for data acquisition and analysis. Summary data are presented as means $\pm$ S.E.M. Full-field, red (667 nm) light stimuli were used to evoke EPSCs and EPSPs. The intensity of the unattenuated light was 7.3×10^9 quanta cm^{-2} s^{-1}, as measured by a photodiode referenced to a calibrated thermopile. A 2 s light stimulus was presented each 30–60 s.

Live/dead assay

Dissociated cells were exposed either for 30 min to 100 μM glutamate (in the presence of 100 μM Cd^{2+}), or for 5 min to modified Ringer solution containing 100 mM KCl, and then washed for 2 h and loaded with fluorescent dyes calcein-AM (2 μM) and ethidium homodimer (4 μM), for 30 min (Live/Dead assay, Molecular Probes). Cells were visualized with laser scanning confocal microscope and counted directly. The percentage number of viable cells (normalized to control value) was calculated as: (number of live cells/total number of cells) $\times$ 100. All data are expressed as the means $\pm$ S.E.M. Significance of differences between groups was assessed by Student's paired t test.

Results

Depolarization-induced F-actin disruption in retinal vertical sections

To investigate depolarization-induced changes in the organization of the actin cytoskeleton, one eyecup was treated with control Ringer solution while the second eyecup (from the same animal) was exposed for 5 min to modified Ringer solution containing 100 mM KCl. Both eyecups were then fixed and stained with Alexa-Fluor488-phalloidin. Under these conditions, the fluorescence intensity of phalloidin, used to stain, visualize and quantify the actin cytoskeleton (Dancker *et al.* 1975), was significantly reduced in the outer plexiform (OPL), the inner plexiform (IPL) and the ganglion cell layer (GCL), indicating that F-actin depolymerization had occurred. Representative confocal images of vertical cryostat sections (from 3 independent experiments), stained after exposure to control Ringer solution or after 5 min incubation with 100 mM KCl, show a depolarization-induced reduction in polymerized actin, as assessed by $60 \pm 5\%$ loss in Alexa-Fluor488-phalloidin intensity (Fig. 1*A*). To make sure that the loss of phalloidin staining was not the result of cell death after high-K$^+$ treatment, we exposed retinal eyecups for 5 min to 100 mM KCl and then washed for 2 h; whole-cell voltage- and light-induced currents were then recorded from ganglion cells in a slice preparation. All cells responded to both voltage and light stimuli (not shown), indicating that they were still viable after exposure to high K$^+$. The disruptive effect of high-K$^+$-induced depolarization on F-actin closely resembled the action of 30 min exposure to 10 μM latrunculin A, an actin-depolymerizing agent (Spector *et al.* 1983). The effect of high K$^+$ on phalloidin intensity was attenuated in the presence of CdCl$_2$ (100 μM), which was applied 5 min prior to and during high-K$^+$ treatment, indicating that Ca^{2+} influx through voltage-gated channels mediated the depolarization-induced F-actin disruption. The L-type Ca^{2+} channel blocker nifedipine (10 μM), applied 5 min before and during high-K$^+$ treatment, eliminated the effect of K$^+$-induced depolarization (not shown). In addition, when experiments were carried out in a nominally Ca^{2+}-free Ringer solution (Ca^{2+} replaced with Mg^{2+}), in the presence of 10 mM EGTA (applied 10 min before and during high-K$^+$ treatment), the disrupting effect of high K$^+$ on F-actin was significantly reduced. Fluorescence intensity profiles of the OPL and the IPL along the white line on each image are illustrated (Fig. 1*B*).

Calcium-induced F-actin depolymerization in dissociated cells

It is usually difficult to observe detailed changes in fluorescence intensity of individual neurons in retinal

sections. Therefore, further experiments were conducted on acutely dissociated cells. In our observations, we focused primarily on large cells (presumed amacrine or ganglion cells) that retained one or more long processes after dissociation, and which were easily distinguished on morphological grounds from photoreceptors, horizontal, bipolar and Müller cells.

To test the effect of depolarization on F-actin organization, we briefly (5 min) exposed dissociated cells to modified Ringer solution containing 20–30 mM KCl and then fixed and stained them with Alexa-Fluor488-phalloidin. Figure 2A illustrates actin filament staining, which outlined the perimeter of the control cell body. Some phalloidin-stained actin filament granules were also detected in the cell's interior. High-K^+-induced depolarization resulted in a loss of polymerized actin, as assessed by very faint phalloidin staining. To quantify the reorganization of the actin cytoskeleton, the intensity profile of F-actin staining along the indicated white lines was determined (Fig. 2B) and averaged for at least 15 cells from three to five independent experiments (each in control and high-K^+ Ringer solution). The cytoskeleton organization in soma was characterized by two prominent peaks of F-actin staining, delineating the submembranous area, and a strong reduction in intensity between two peaks representing the interior of the cells. As observed in the vertical sections, block of voltage-activated Ca^{2+} channels by $CdCl_2$ (100 μM), applied 5 min before and during the 5 min exposure to high K^+, or removal of

external free Ca^{2+} by EGTA (10 mM, applied 10 min before and during 5 min exposure to high K^+), attenuated a disruptive effect of depolarization on F-actin (not illustrated). Quantitative analysis revealed a $53 \pm 5\%$ ($n = 23$, $P < 0.001$) reduction in phalloidin fluorescence intensity in cells treated with high K^+ compared to untreated cells. In contrast, the mean reduction in fluorescence intensity elicited by depolarization in the presence of Cd^{2+} and EGTA were $4 \pm 5\%$ ($n = 17$, n.s.), and $5 \pm 5\%$ ($n = 20$, n.s.), respectively (Fig. 2C). Sincee a block of Ca^{2+} channels by Cd^{2+} eliminated depolarization-induced F-actin disruption, we next tested the specific contribution of high-voltage-activated N- and L-type channels. Dissociated cells were treated for 5 min with control Ringer solution containing 5 μM nifedipine, and then exposed for 5 min to high-K^+ solution (in the continuous presence of nifedipine), prior to fixing and staining with Alexa-Fluor488-phalloidin. Blockade of L-type channels by nifedipine sharply attenuated the effect of depolarization, resulting in only $10 \pm 6\%$ ($n = 15$, $P > 0.5$) reduction in phalloidin intensity. In contrast, similar treatment with ω-conotoxin GVIA (1 μM), which blocks N-type Ca^{2+} channels, had no effect, since high K^+ still reduced the fluorescence intensity of phalloidin staining by $50 \pm 5\%$ ($n = 15$, $P < 0.001$). The bar graph in Fig. 2C (lower panel) summarizes these results. Neither of these agents applied in control Ringer solution had any significant effect on the intensity of phalloidin staining ($n = 10$, not shown). These data, combined with those observed in retinal
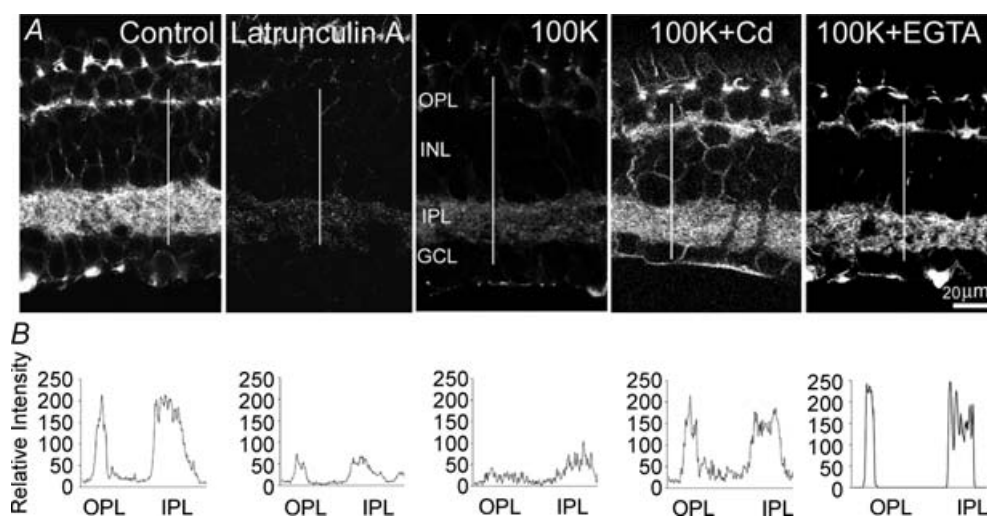

Figure 1. Distribution of F-actin in control and depolarized retina
A, confocal fluorescence images of F-actin distribution in the vertical cryostat sections of retina treated with control Ringer solution (Control), after 30 min incubation with 1 μM latrunculin A, after 5 min exposure to modified Ringer solution containing 100 mM KCl alone (100K), or in combination with 100 μM $CdCl_2$ (100K+Cd) or 10 mM EGTA (100K+EGTA). Phalloidin fluorescence intensity profiles across the line from the outer border of the OPL to inner boarder of the IPL in each experimental condition are illustrated (B). OPL, outer plexiform layer; INL, inner nuclear layer; IPL, inner plexiform layer; GCL, ganglion cell layer.

sections, indicate that depolarization-induced Ca^{2+} influx through high-voltage-activated L-type channels results in actin depolymerization in salamander retinal cells.

The involvement of PKC in Ca^{2+}-induced F-actin depolymerization

Increasing lines of evidence indicate that classical and novel isoforms of PKC have significant roles in regulating cytoskeleton-driven processes (reviewed by Keenan & Kelleher, 1998; Larsson, 2006). We used PKC antagonists to determine whether it is involved in the Ca^{2+}-induced F-actin disruption. Chelerythrine and GF 109203X are highly specific PKC antagonists with a > 100-fold selectivity for PKC over either protein kinase A or calcium–calmodulin-dependent protein kinase (Herbert *et al.* 1990). To assess the ability of these agents to interfere with the depolarization-induced F-actin changes, dissociated cells were first incubated for 20 min in control Ringer solution containing either $50\,\mu M$ chelerythrine or $1\,\mu M$ GF 109203X, then for 5 min with modified solution containing 20 mM KCl in the continuous presence of PKC antagonist, before fixing

and staining with Alexa-Fluor488-phalloidin. Figure 3*A* shows confocal fluorescence images of cells stained with Alexa-Fluor488-phalloidin in control Ringer solution, in modified solution containing 20 mM KCl alone, or in solution containing 20 mM KCl combined with either chelerythrine or GF 109203X. As observed by confocal laser scanning microscope analysis, both PKC antagonists attenuated a depolarization-induced F-actin disruption. The mean reduction in phalloidin fluorescence intensity induced by high K^+ was $12 \pm 13\%$ ($n = 13$; $P > 0.5$) and $3 \pm 8\%$ ($n = 15$; $P > 0.5$) in cells pretreated with chelerythrine or GF 109203X, respectively, compared to a $63 \pm 8\%$ ($n = 28$; $P < 0.001$) reduction observed in cells treated with high K^+ alone. Neither of these agents had any significant effect on F-actin when applied alone in control Ringer solution ($n = 15$, not illustrated). Further evidence for the involvement of PKC activation was provided by the use of the phorbol ester, phorbol 12-myristate 13-acetate (PMA), which activates PKC in a Ca^{2+}-independent manner (Mosior & Newton, 1996). Exposure of cells for 20 min to control Ringer solution containing $0.5\,\mu M$ PMA resulted in a loss of F-actin, as assessed by a $56 \pm 6\%$ ($n = 20$; $P < 0.001$) reduction
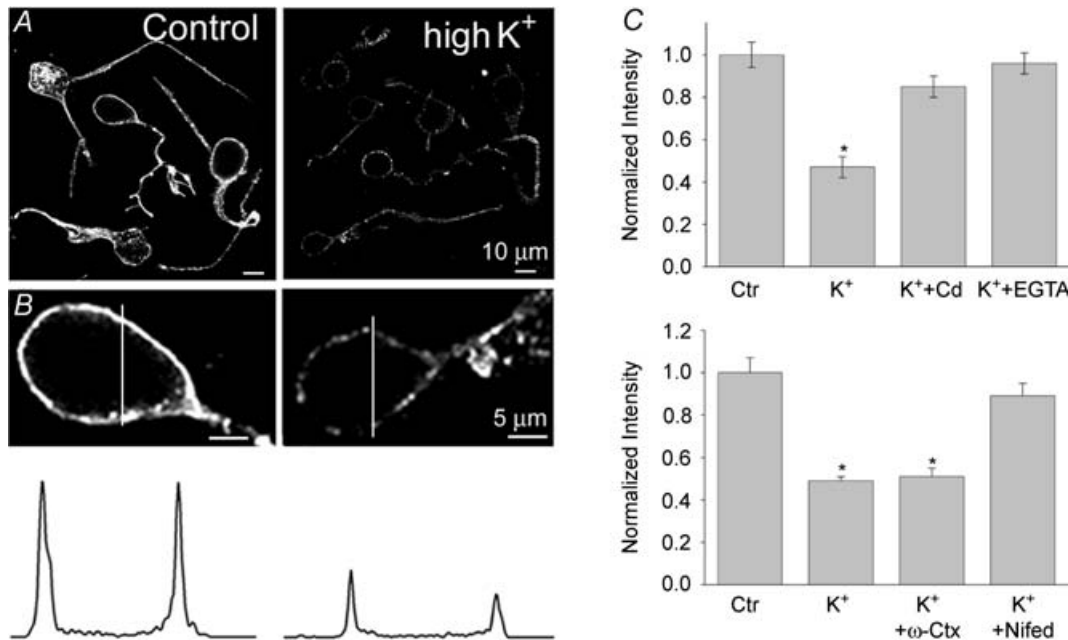

Figure 2. A depolarization-induced change in F-actin organization in retinal neurons is mediated by Ca^{2+} influx through L-type channels
A, cells are stained with Alexa-Fluor488-phalloidin treated either in control Ringer solution (Control) or after 5 min exposure to modified Ringer solution containing 20 mM KCl (high K^+). Magnified fluorescence confocal images of cell bodies and corresponding fluorescence intensity profiles across the indicated white lines are illustrated for control and high-K^+-treated cells (*B*). *C*, the bar charts summarize the effects of $100\,\mu M$ Cd^{2+} and 10 mM EGTA on high-K^+-induced F-actin disruption. Nifedipine ($10\,\mu M$), but not ω-conotoxin GVIA ($1\,\mu M$) attenuated the disrupting effect when applied together with high K^+. The change in F-actin content is expressed as a relative change in the mean phalloidin fluorescence intensity, and the fluorescence intensity of untreated control cells is expressed as 1. Quantification of F-actin changes was performed based on at least 15 cells from 3 independent experiments and the means $\pm$ S.E.M. are shown. *$P < 0.0001$ compared to control values.

in phalloidin fluorescence intensity. Similar treatment with 4α-PMA (0.5 μM), an inactive PMA analogue, was ineffective ($n = 10$; not illustrated). Fluorescence intensity profiles of corresponding cells across the marked white line are illustrated (Fig. 3*B*). The bar graph in Fig. 3*C* summarizes these results indicating that PKC plays a critical role in Ca^{2+}-induced F-actin depolymerization in retinal neurons.

Effect of the other sources of Ca^{2+} on F-actin

We next tested whether a rise in the intracellular Ca^{2+} concentration that triggers F-actin disruption results specifically from Ca^{2+} entering the cell through voltage-gated channels or may also result either from Ca^{2+} entry through glutamate receptor-activated channels or from Ca^{2+} being released from intracellular stores. In salamander third-order retinal neurons, activation of ionotropic glutamate receptors is associated with

a Ca^{2+} influx (Shen & Slaughter, 1999; Akopian *et al.* 2006). To examine the effect of Ca^{2+} entry through glutamate receptors, cells were incubated for 30 min in Ringer solution containing 100 μM glutamate and 100 μM $CdCl_2$ (to exclude Ca^{2+} entry through voltage-gated channels), prior to fixing and staining with Alexa-Fluor488-phalloidin. Blockade of voltage-gated Ca^{2+} channels will also significantly prevent excitotoxicity in cells caused by glutamate (Sucher *et al.* 1997). In these conditions, glutamate caused a disruption of F-actin in the perimeter of cell somata (Fig. 4*B*) as assessed by a reduction in the intensity of phalloidin staining around the soma. A significant change in pattern of phallodin staining (described below) was observed in processes. Quantification revealed a $34 \pm 6\%$ ($n = 35$, $P < 0.001$) reduction in fluorescence intensity of phalloidin in the submembranous area of cells treated with glutamate. Intensity profiles in cell somata and processes along the indicated white lines are illustrated in the inset of
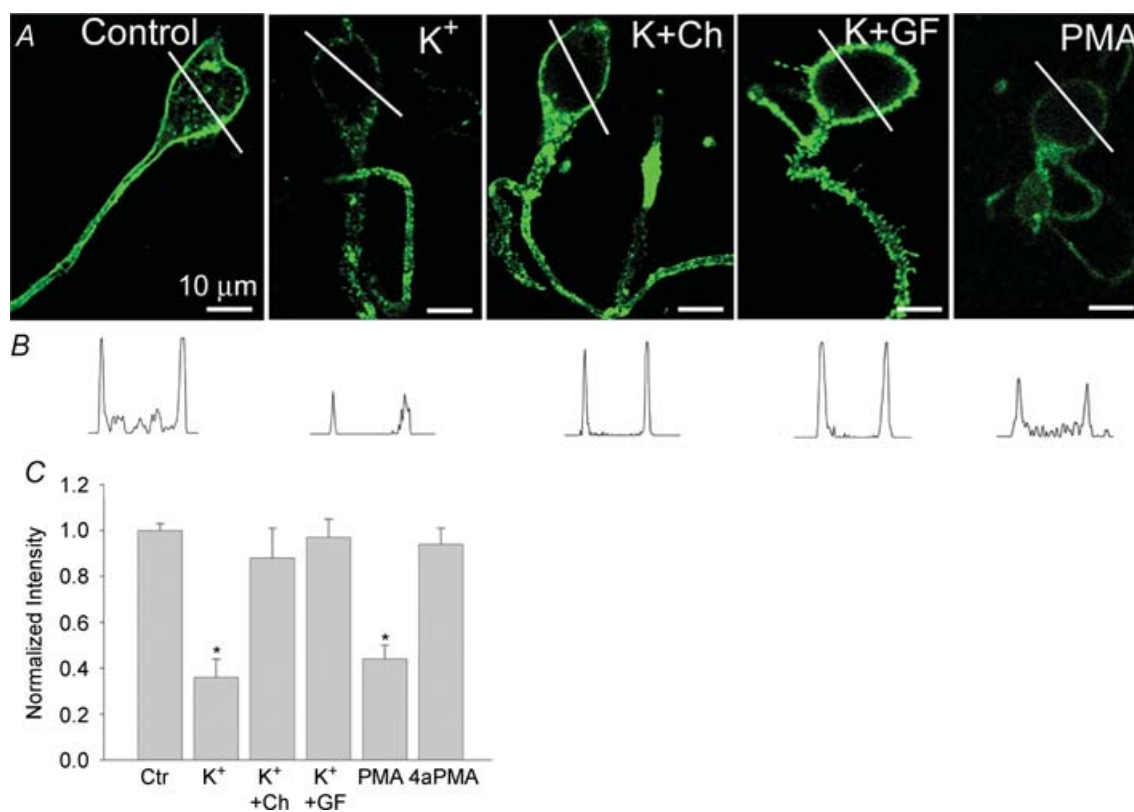

Figure 3. Inhibitors of PKC attenuate Ca^{22+}-induced F-actin depolymerization
A, confocal fluorescence images of F-actin distribution in cells treated with control Ringer solution (control), after depolarization with 20 mM KCl alone (K^+), or in combination with either 50 μM chelerythrine (K+Ch) or 1 μM GF 109203X (K+GF), then fixed and stained with Alexa-Fluor488-phalloidin. PMA (0.5 μM) was applied to the control Ringer solution for 20 min prior to staining with phalloidin. *B*, intensity profiles of phalloidin staining for each cell across the marked white lines are illustrated. *C*, bar graph summarizing effects of PKC antagonists on Ca^{2+}-induced F-actin depolymerization. Values represent mean fluorescence intensity and s.e.m. Data are based on 15–20 cells from 3–5 independent experiments. *$P < 0.0001$ compared to control values.

each image. To determine the type(s) of ionotropic glutamate receptor involved in F-actin disruption, we treated cells separately with AMPA (50 μM, in normal medium) and NMDA (100 μM, in Mg^{2+}-free medium) for 10–15 min, then fixed and stained the cells with Alexa-Fluor488-phalloidin. Activation of either AMPA or NMDA receptors resulted in a reduction of phalloidin fluoresence intensity by $42 \pm 6\%$ ($n = 24$, $P < 0.01$) and $31 \pm 9\%$ ($n = 24$, $P < 0.01$), respectively, compared to control cells. In some cells (Fig. 4C and C'), treatment with NMDA had little effect on the intensity of phalloidin staining in the cell soma, but caused a dramatic change in the pattern of staining in processes. In contrast to control cell processes, where pronounced phalloidin-positive labelling of the submembranous area and a more diffuse, granular staining within the cytoplasmic compartment was observed (Fig. 4A'), cells treated with glutamate agonists displayed a much reduced intensity of phalloidin labelling along the membrane and more intense fluorescent patches in the centre of the dendritic shaft (Fig. 4B', C' and D'). Changes in phalloidin staining could be the result of permanent damage to cells caused by glutamate excitotoxicity. In our experiments, we applied 100 μM Cd^{2+} to exclude any contribution from voltage-gated Ca^{2+} channels, which would also significantly reduce glutamate-induced excitotoxicity (Sucher *et al.* 1997). Nevertheless, to exclude this possibility, dissociated cells were treated with 100 μM glutamate for 30 min and then washed for 2 h with normal Ringer solution, and whole-cell

voltage-gated currents were recorded from cells with a smooth appearance of soma and intact processes. All cells ($n = 10$) generated currents in response to depolarizing voltage steps from -50 to $+30$ mV evoked from a holding potential of -70 mV (not shown). The bar graph in Fig. 4E summarizes the effects of ionotropic glutamate receptor activation on F-actin organization.

We next tested the possible effect of a rise in intracellular Ca^{2+} released from intracellular stores on F-actin. In the first series of experiments, retina was treated with caffeine, which stimulates Ca^{2+} release from ryanodine-sensitive stores. Cells were treated with Ringer solution containing 10 mM caffeine for 5–10 min prior to fixing and staining with Alexa-Fluor488-phalloidin. Caffeine had no effect on the intensity of phalloidin staining ($n = 5$, not shown). Lack of an effect of caffeine on actin organization in our study might result from a small and transient rise in intracellular Ca^{2+}, in contrast to the sustained rise in Ca^{2+} evoked by high K^{+} (Krizaj *et al.* 2003), which might therefore not be sufficient to depolymerize actin filaments. In the next approach, we stimulated Ca^{2+} release by incubating dissociated cells for 20–30 min with thapsigargin (1 μM in Ringer solution) prior to phalloidin staining. Thapsigargin also had no effect on phalloidin fluorescence intensity ($n = 10$; not illustrated). These data indicate that, in contrast to Ca^{2+} influx through voltage- and glutamate-activated channels, the Ca^{2+} released from internal stores is unable to affect actin organization, suggesting a crucial role for a source of intracellular [Ca^{2+}] elevation for its action.
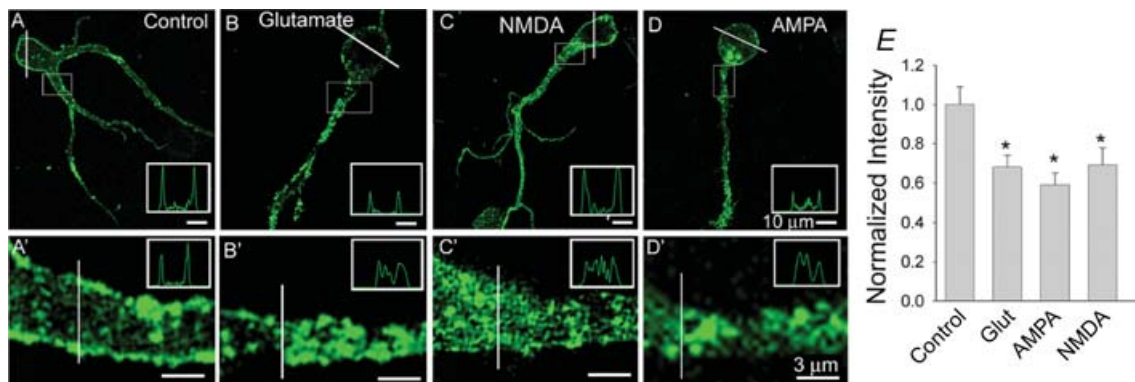

Figure 4. Activation of glutamate receptors causes F-actin disruption in third-order retinal neurons
Confocal fluorescence images of cells incubated in the absence (*A*) or presence (*B*) of 100 μM glutamate in control Ringer solution for 30 min, with 100 μM NMDA (in Mg^{2+}-free medium) for 10 min (*C*) or 50 μM AMPA for 10 min (*D*) prior to fixing and staining with Alexa-Fluor488-phalloidin. Glutamate and its agonists were applied in the presence of 100 μM CdCl$_2$. Panels *A'–D'* show magnified fluorescence images of the dendritic region adjacent to cell somata shown in panels *A–D*, as indicated by the boxes. Fluorescence intensity profiles across the indicated white lines for individual cell somata and dendrites are illustrated (insets). Note that cells treated with glutamate agonists displayed reduced intensity of phalloidin labelling along the membrane and more discrete fluorescent patches inside the dendritic shaft compared to control cells. *E*, bar graph summarizing the effect of ionotropic glutamate receptor agonists on F-actin content. Values represent the mean phalloidin fluorescence intensity and s.e.m. measured in at least 25 cells from 3 independent experiments. *$P < 0.05$ compared to control values.

Viability of cells treated with glutamate and high K$^+$

To assure that changes in phalloidin fluorescence intensity was not associated with cell death caused by various treatments (high K$^+$, glutamate), we conducted two-dye colour live/dead assay on dissociated cells treated and subsequently washed for 2 h. For comparison, control cells were loaded with dyes following 2 h incubation in control Ringer solution. Viable cells were labelled by the green fluorescence generated by the esterase hydrolysis of a membrane-permeant dye, calcein-AM. Dead cells were marked by the red fluorescence of a membrane-impermeant DNA marker, ethidium homidimer. The results of three separate experiments (each provided in duplicate), showed that, compared to control cells, 78 ± 2% of glutamate-treated cells and 88 ± 2% of KCl-treated cells were viable (Fig. 5*A*, *B* and *C*). The bar graph in Fig. 5*D* summarizes the percentage number of viable cells in each experimental condition. As a further test of the fluorescence viability assay, whole-cell currents were measured in treated dissociated cells and slices. All recorded cells exhibited voltage-gated currents and light-induced EPSCs characteristic of normal functional cells. The results indicate that in the presence of Ca^{2+} channel blocker (Cd^{2+} in the external solution), glutamate-induced cell damage was relatively low and that changes in phalloidin fluorescence intensity was not associated with cell death.

Implication in the regulation of light-evoked EPSCs

Postsynaptic actin serves as a key mediator between structural plasticity and signal transmission at excitatory synapses (reviewed by Matus, 1999; Dillon & Goda, 2005). The disruption of F-actin by glutamate-induced Ca^{2+} influx (present study) and the subsequent effect of actin depolymerization on Ca^{2+} influx through glutamate receptor-activated channels (Akopian *et al.* 2006) prompted us to examine the possible physiological significance of these findings. We tested whether glutamatergic synaptic responses were affected by the actin cytoskeleton reorganization. In a slice preparation, 'on–off' ganglion cells were held at −70 mV, and whole-cell EPSCs in response to 2 s light stimulation were recorded with the patch pipette containing either latrunculin B (5 μM) or cytochalasin B (10 μM). To assess the effect of F-actin disruption, EPSCs were recorded within 1 min of membrane rupture and after 30 min incubation with latrunculin B (Fig. 6*A*). A disruption of F-actin resulted in a 60 ± 8% ($n = 8$, $P < 0.01$) reduction in 'off' EPSCs, remarkably having no significant effect on 'on' EPSCs. In contrast, similar treatment with colchicine (50 μM), a microtubule-disrupting agent, had no significant effect on either 'on' or 'off' EPSCs ($n = 4$). Whole-cell recordings in current-clamp mode revealed qualitatively similar attenuation of light-evoked 'off' EPSPs by latrunculin B, without significant changes in 'on' EPSPs. In the cell
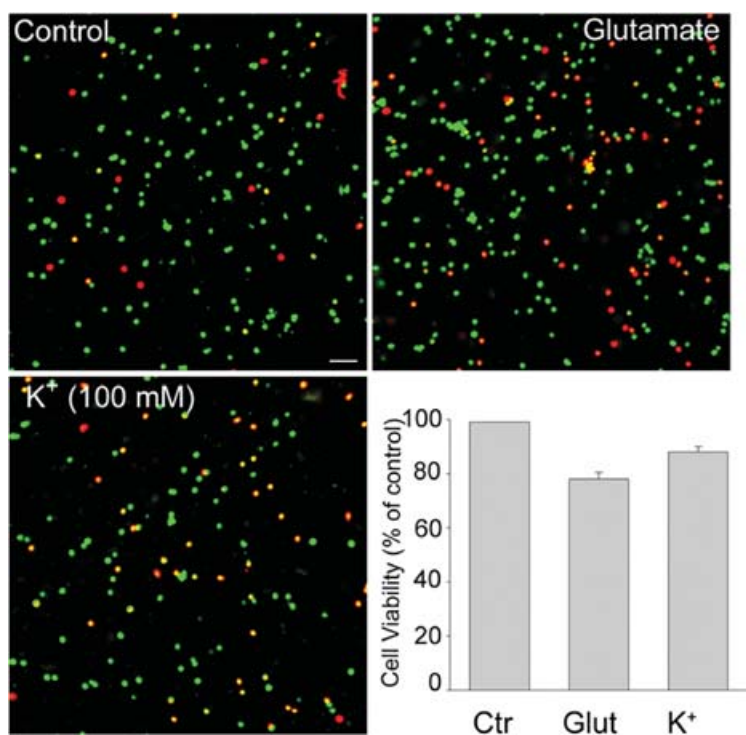

Figure 5. Live/dead fluorescence assay of dissociated cells
Confocal images of dissociated cells treated with either 100 μM glutamate (for 30 min; *B*), or 100 mM KCl (for 5 min; *C*) and subsequently washed for 2 h before double labelling with the fluorescent dyes ethidium homodimer (red) and calcein-AM (green). Control cells (*A*) were labelled after 2 h incubation in control Ringer solution. Viable cells were marked by green fluorescence, whereas dead cells were marked by red fluorescence. *D*, bar graph represents cell viability (% of control) calculated from 3 separate experiments. The ratios of live cells to total cells (viability) were determined for control and treated cells by directly counting 300–600 cells in randomly chosen microscopic fields of each sample. All data represent means + s.e.m. Calibration bar, 100 μm.

illustrated in Fig. 6*B*, a longer (60 min) incubation with latrunculin B resulted in a complete inhibition of the 'off' EPSPs with only a slight reduction in the 'on' EPSPs. The bar graph in Fig. 6*C* summarizes the effect of actin depolymerization on the amplitudes of light-evoked 'on' and 'off' EPSCs in retinal ganglion cells.

Discussion

The principal finding of our study is that in salamander inner retinal neurons, Ca^{2+} influx through high-voltage-activated L-type channels causes F-actin depolymerization, and PKC activation plays a critical role in this process.

The importance of the relationship between Ca^{2+} and the cytoskeletal architecture in the vertebrate retina stems from the role that Ca^{2+} plays in signal transduction, and in its regulation of numerous cellular processes through the activation of multiple intracellular cascades (reviewed by Akopian & Witkovsky, 2002; Krizaj &

Copenhagen, 2002). Thus, in salamander retina, intracellular Ca^{2+} elevation through diverse sources, including influx through L-type channels, regulates the activity of GABA receptors in ganglion cells (Shen & Slaughter, 1999), closes non-selective cation channels activated by mGluR6 in bipolar cells (Nawy, 2000), reduces the light-evoked EPSCs in ganglion cells (Akopian & Witkovsky, 2001) and appears to play an important role in mediating transmitter release in amacrine cells (Bieda & Copenhagen, 2004). Calcium influx from different sources induces diverse changes in actin cytoskeleton organization that in some cases are difficult to reconcile or even appear contradictory (Oertner & Matus, 2005). We found that Ca^{2+} influx through voltage- and glutamate-activated channels, but not by release from internal stores, caused F-actin disruption. Quantification of F-actin on cell somata revealed a much stronger (∼60%) disruption when Ca^{2+} entered through voltage-gated channels compared to glutamate receptor-activated channels (30–40%). At the same time, more dramatic changes in the pattern
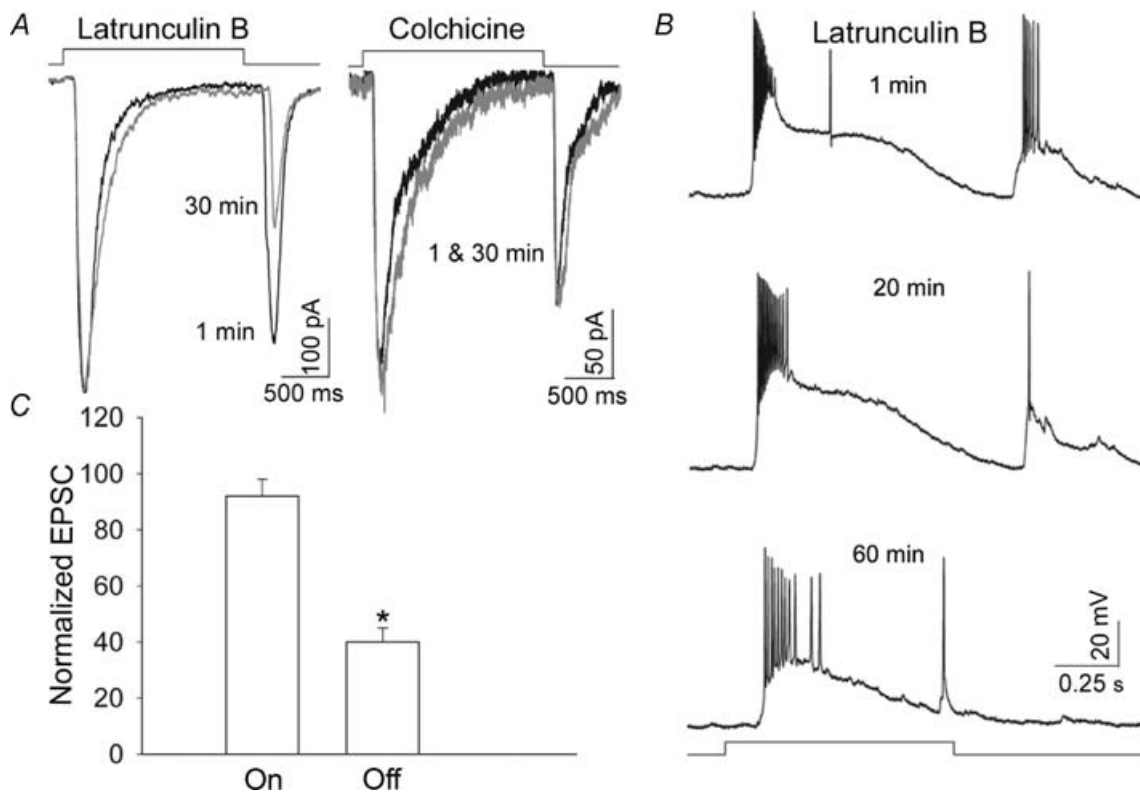

Figure 6. Regulation of the light-evoked EPSCs by actin cytoskeleton in 'on–off' ganglion cells
A, F-actin depolymerization by latrunculin B caused a reduction in 'off' but not 'on' EPSCs. In contrast, disruption of microtubules by colchicine had no effect on either type of EPSCs. Traces shown are recorded within 1 min of membrane rupture (black lines) and after 30 min in the whole-cell configuration (grey lines) with the patch pipette containing either 5 μM latrunculin B or 50 μM colchicine. *B*, in current clamp mode, F-actin disruption by latrunculin B resulted in a dramatic reduction in 'off' EPSPs but only a small effect on 'on' EPSPs. *C*, bar graph summarizes the effect of 30 min incubation with cytochalasin B on 'on' and 'off' EPSCs. Values represent the mean and s.e.m. of determinations made in 8 cells in three separate preparations. *$P < 0.01$ compared to values obtained within 1 min of membrane rupture.

of phalloidin staining by glutamate receptor agonists was observed in the cell processes (Fig. 4*B′*, *C′* and *D′*), where fluorescence appears as discrete patches inside the dendritic shaft, compared to more continuous labelling along the membrane in control cells (Fig. 4*A′*). This may reflect the higher amount of Ca^{2+} entering through voltage-gated L-type channels, which are densely localized on the surface of cell somata (M. Cristofanilli & A. Akopian, unpublished observation), compared to the amount of Ca^{2+} influx stimulated by AMPA or NMDA, whose receptors are preferentially expressed by amacrine and ganglion cell dendrites (Grunert *et al.* 2002). In addition, the greater effect of Ca^{2+} influx through voltage-gated channels may reflect a longer time available for Ca^{2+} entry through sustained L-type channels compared to desensitizing glutamate receptors. Alternatively, the temporal and spatial regulation of intracellular $[Ca^{2+}]$ may also be critical for cytoskeleton rearrangement. The fact that Ca^{2+} release from internal stores had no effect on actin organization supports this idea. A multiple spatiotemporal mode of actin reorganization by NMDA receptors and voltage-gated Ca^{2+} channels has been demonstrated in hippocampal neurons (Furuyashiki *et al.* 2002).

The idea that PKC could be an important regulator of cytoskeletal organization has been supported by numerous studies (reviewed by Larsson, 2006). Block of Ca^{2+}-induced F-actin disruption in the presence of specific PKC inhibitors suggests that the PKC activation mediates the effect of Ca^{2+} entering through voltage-gated channels. Our results are consistent with those observed in other cell types, in which the activation of PKC has been shown to mediate actin depolymerization (Schliwa *et al.* 1984; Brandt *et al.* 2002), but contrast strikingly with the Ca^{2+}- and PKC-mediated polymerization of F-actin in bipolar cell terminals of the goldfish retina (Job & Lagnado, 1998). The reason for such apparent discrepancy might be the differential localization and expression of distinct isoenzymes of protein kinase C in the retina (Kosaka *et al.* 1998; Fyk-Kolodziej *et al.* 2002), and the family of substrate proteins that have been suggested as candidates for mediating PKC effects on the cytoskeleton (reviewed by Larsson, 2006). These substrates include a group of actin-binding proteins that link actin with the surface membrane and promote diverse changes in actin filament structure when phosphorylated by PKC (reviewed by Keenan & Kelleher, 1998; Calabrese & Halpain, 2005). In general, classical (PKC_α, $_{\beta I}$, $_{\beta II}$ and $_\gamma$), and novel isoforms (PKC_ε, $_\delta$, $_\eta$, and $_\theta$) both contain binding domains for phorbol esters, whereas only the classic isoforms contain a domain for Ca^{2+} binding (Larsson, 2006). The fact that the PKC antagonists, chelerythrine and GF 109230X, attenuated the effect of depolarization-induced Ca^{2+} influx on F-actin disruption, and that PMA mimicked this effect in the absence of

KCl-induced depolarization, suggests an involvement of both Ca^{2+}-dependent and -independent pathways of cytoskeleton regulation by PKC in retinal neurons. In contrast, only the PKC_α (Ca^{2+}-dependent) isoform is expressed in the synaptic terminals of depolarizing bipolar cells, and no other isoform of PKC was detected (Osborne *et al.* 1992). Accordingly, in this preparation, phorbol esters had no effect on actin network in the absence of depolarization-induced Ca^{2+} influx (Job & Lagnado, 1998). The lack of a common effect of PKC on F-actin in different cells suggests that a wide range of pathways may mediate the PKC effect, including direct phosphorylation of cytoskeletal regulators and influence on other intracellular signalling pathways.

Two major proteins that mediate Ca^{2+}-dependent changes in the actin cytoskeleton, namely gelsolin (Forscher, 1989; Furukawa *et al.* 1997) and myristoylated alanine-rich C kinase substrate (MARCKS; Arbuzova *et al.* 2002), might be involved in Ca^{2+}-induced actin depolymerization. There is an apparent link between PKC activation and function of these proteins. That is, antagonists of PKC have been shown to inhibit the induction of galsolin in Human Leulzemia (HL)60 cells (Miyamoto & Wu, 1990), whereas phosphorylation of MARCKS, an F-actin cross-linking protein, by PKC induced spine loss and shrinkage, accompanied by a reduced F-actin content in hippocampal neurons (Calabrese & Halpain, 2005). We observed anti-gelsolin immunoreactivity in cell bodies in the inner nuclear layer and the ganglion cell layer of salamander retina (M. Cristofanilli and A. Akopian, unpublished observations), but whether gelsolin is involved in Ca^{2+}-induced F-actin depolymerization in the retina remains to be determined.

The contribution of the actin cytoskeleton to the regulation of synaptic transmission and plasticity has been a matter of extensive study in recent years (reviewed by Dillon & Goda, 2005). Disruption of postsynaptic F-actin (latrunculin B applied to the patch pipette) in our study caused a significant reduction in light-evoked 'off' EPSCs, remarkably having no effect on 'on' EPSCs in 'on–off' ganglion cells. We did not investigate mechanism(s) underlying the selective regulation of 'off' EPSCs by F-actin, since it was beyond the scope of the present study. It is possible, however, that the regulatory pathways involving different kinases and their substrates, a group of actin-binding proteins that promote diverse changes in actin filament structure when phosphorylated, are different for receptors in sublaminae 1 and 5, where 'on–off' ganglion cell processes are stratified. Disruption of microtubules with colchicines, in contrast, had no effect on either 'on' or 'off' EPSCs, indicating that in the vertebrate retina, as in the hippocampus, the actin cytoskeleton plays an important role in the regulation of excitatory postsynaptic responses. Further studies are needed

to explore the mechanism(s) underlying cytoskeletal regulation of synaptic responses and the role of various enzymes and actin-binding proteins in the retina.

Physiological implications

In the vertebrate retina, actin reorganization causes a variety of structural (Mandell *et al.* 1993; Weiler & Janssen-Bienhold, 1993; Job & Lagnado, 1998; Gallo *et al.* 2002) and functional changes (Maguire *et al.* 1998; Schmidt, 2004). Our data suggest that the activity-dependent increase of postsynaptic Ca^{2+} levels beyond a particular threshold may trigger a disruption of actin filaments, which in turn will tend to reduce the Ca^{2+} influx through voltage-activated (Schubert & Akopian, 2004) or glutamate receptor-activated channels (Akopian *et al.* 2006), thereby influencing the light-evoked excitatory postsynaptic responses (present study). For example, the build up of internal Ca^{2+} resulting from the light-'on' response might initiate F-actin disruption and subsequent reduction in the 'off' response. Depending on the source of Ca^{2+} increase, the result may be the local, and transient or long-lasting changes in F-actin organization and postsynaptic cell function. Calcium-dependent cytoskeleton reorganization observed in our study may also underlie the mechanism of Ca^{2+}-induced Ca^{2+} inactivation (Johnson & Byerly, 1993).

Taking together, our data suggest a reciprocal relationship between glutamate receptors, Ca^{2+} and F-actin in regulating synaptic function in the salamander retina. Such a relationship may underlie a negative feedback pathway, which serves to attenuate the excessive intracellular Ca^{2+} accumulation that plays a primary role in excitotoxicity, a form of neuronal injury caused by overstimulation of glutamate receptors (Sucher *et al.* 1997).

References

Akopian A, Szikra T, Cristofanilli M & Krizaj D (2006). Glutamate-induced Ca^{2+} influx in third-order neurons of salamander retina is regulated by the actin cytoskeleton. *Neuroscience* **138**, 17–24.

Akopian A & Witkovsky P (2001). Intracellular calcium reduces light-induced excitatory post-synaptic responses in salamander retinal ganglion cells. *J Physiol* **532**, 43–53.

Akopian A & Witkovsky P (2002). Calcium and retinal function. *Mol Neurobiol* **25**, 113–132.

Arbuzova A, Schmitz AA & Vergeres G (2002). Cross-talk unfolded: MARCKS proteins. *Biochem J* **362**, 1–12.

Bieda MC & Copenhagen DR (2004). N-Type and L-type calcium channels mediate glycinergic synaptic inputs to retinal ganglion cells of tiger salamanders. *Vis Neurosci* **21**, 545–550.

Brandt D, Gimona M, Hillmann M, Haller H & Mischak H (2002). Protein kinase C induces actin reorganization via a Src- and Rho-dependent pathway. *J Biol Chem* **277**, 20903–20910.

Brunig I, Kaech S, Brinkhaus H, Oertner TG & Matus A (2004). Influx of extracellular calcium regulates actin-dependent morphological plasticity in dendritic spines. *Neuropharmacology* **47**, 669–676.

Calabrese B & Halpain S (2005). Essential role for the PKC target MARCKS in maintaining dendritic spine morphology. *Neuron* **48**, 77–90.

Chittajallu R, Alford S & Collingridge GL (1998). Ca^{2+} and synaptic plasticity. *Cell Calcium* **24**, 377–385.

Dancker P, Low I, Hasselbach W & Wieland T (1975). Interaction of actin with phalloidin: polymerization and stabilization of F-actin. *Biochim Biophys Acta* **400**, 407–414.

Dillon C & Goda Y (2005). The actin cytoskeleton: integrating form and function at the synapse. *Annu Rev Neurosci* **28**, 25–55.

Forscher P (1989). Calcium and polyphosphoinositide control of cytoskeletal dynamics. *Trends Neurosci* **12**, 468–474.

Furukawa K, Fu W, Li Y, Witke W, Kwiatkowski DJ & Mattson MP (1997). The actin-severing protein gelsolin modulates calcium channel and NMDA receptor activities and vulnerability to excitotoxicity in hippocampal neurons. *J Neurosci* **17**, 8178–8186.

Furukawa K, Smith-Swintosky VL & Mattson MP (1995). Evidence that actin depolymerization protects hippocampal neurons against excitotoxicity by stabilizing $[Ca^{2+}]_i$. *Exp Neurol* **133**, 153–163.

Furuyashiki T, Arakawa Y, Takemoto-Kimura S, Bito H & Narumiya S (2002). Multiple spatiotemporal modes of actin reorganization by NMDA receptors and voltage-gated Ca^{2+} channels. *Proc Natl Acad Sci U S A* **99**, 14458–14463.

Fyk-Kolodziej B, Caj W & Pourcho RG (2002). Distribution of protein kinase C isoforms in the cat retina. *Vis Neurosci* **19**, 549–562.

Gallo G, Yee HF & Letourneau PC (2002). Actin turnover is required to prevent axon retraction driven by endogenous actomyosin contractility. *J Cell Biol* **158**, 1219–1228.

Grunert U, Haverkamp S, Fletcher EL & Wassle H (2002). Synaptic distribution of ionotropic glutamate receptors in the inner plexiform layer of the primate retina. *J Comp Neurol* **447**, 138–151.

Halpain S, Hipolito A & Saffer L (1998). Regulation of F-actin stability in dendritic spines by glutamate receptors and calcineurin. *J Neurosci* **18**, 9835–9844.

Herbert JM, Augerean JM, Gleye J & Maffrard JP (1999). Chelerythrine is a patent and specific inhibitor of protein kinase C. *Biochem Biophys Res Commun* **172**, 993–999.

Job C & Lagnado L (1998). Calcium and protein kinase C regulate the actin cytoskeleton in the synaptic terminal of retinal bipolar cells. *J Cell Biol* **143**, 1661–1672.

Johnson BD & Byerly Y (1993). A cytoskeletal mechanism for Ca^{2+} channel metabolic dependence and inactivation by intracellular Ca^{2+}. *Neuron* **10**, 797–804.

Keenan C & Kelleher D (1998). Protein kinase C and the cytoskeleton. *Cell Signal* **10**, 225–232.

Kosaka J, Suzuki A, Morii E & Nomura S (1998). Differential localization and expression of alpha and beta isoenzymes of protein kinase C in the rat retina. *J Neurosci Res* **54**, 655–663.

Krizaj D & Copenhagen DR (2002). Calcium regulation in photoreceptors. *Front Biosci* **7**, 2023–2044.

Krizaj D, Lai FA & Copenhagen DR (2003). Ryanodine stores and calcium regulation in the inner segments of salamander rods and cones. *J Physiol* **547**, 761–774.

Larsson C (2006). Protein kinase C and the regulation of the actin cytoskeleton. *Cell Signal* **18**, 276–284.

Lau P, Zucker RS & Bentley D (1999). Induction of filopodia by direct local elevation of intracellular calcium ion concentration. *J Cell Biol* **145**, 1265–1275.

Maguire G, Connaughton V, Prat AG, Jackson GR & Cantiello HR (1998). Actin cytoskeleton regulates ion channel activity in retinal neurons. *Neuroreport* **9**, 665–670.

Mandell JW, MacLeish PR & Townes-Anderson E (1993). Process outgrowth and synaptic varicosity formation by adult photoreceptors in vitro. *J Neurosci* **13**, 3533–3548.

Matus A (1999). Postsynaptic actin and neuronal plasticity. *Curr Opid Neurobiol* **9**, 561–565.

Miyamoto S & Wu JM (1990). Effect of staurosporine on the induction of actin/gelsolin in PMA-treated HL-60 cells. *Biochem Int.* **22**, 427–433.

Mosior M & Newton AC (1996). Calcium-independent binding to interfacial phorbol esters causes protein kinase C to associate with membranes in the absence of acidic lipids. *Biochemistry* **35**, 1612–1623.

Nawy S (2000). Regulation of the on bipolar cell mGluR6 pathway by Ca^{2+}. *J Neurosci* **20**, 4471–4479.

Neely MD & Gesemann D (1994). Disruption of microfilaments in growth cones following depolarization and calcium influx. *J Neurosci* **14**, 7511–7520.

Oertner TG & Matus A (2005). Calcium regulation of actin dynamics in dendritic spines. *Cell Calcium* **37**, 477–482.

Osborne NN, Barnett NL, Morris NJ & Huang FL (1992). The occurrence of three isoenzymes of protein kinase C (α, β and γ) in retinas of different species. *Brain Res* **570**, 161–166.

Rosenmund C & Westbrook G (1993). Calcium-induced actin depolymerization reduces NMDA channel activity. *Neuron* **10**, 805–814.

Schliwa M, Nakamura T, Porter KR & Euteneuer U (1984). A tumor promoter induces rapid and coordinated reorganization of actin and vinculin in cultured cells. *J Cell Biol* **99**, 1045–1059.

Schmidt JT (2004). Activity-driven sharpening of the retinotectal projection: the search for retrograde synaptic signaling pathways. *J Neurobiol* **59**, 114–133.

Schubert T & Akopian A (2004). Actin filaments regulate voltage-gated ion channels in salamander retinal ganglion cells. *Neuroscience* **125**, 583–590.

Shen W & Slaughter MM (1999). Internal calcium modulates apparent affinity of metabotropic GABA receptors. *J Neurophysiol* **82**, 3298–3306.

Spector I, Shochet NR, Kashman Y & Groweiss A (1983). Latrunculins: novel marine toxins that disrupt microfilament organization in cultured cells. *Science* **219**, 493–495.

Sucher NJ, Lipton SA & Dryer EB (1997). Molecular basis of glutamate toxicity in retinal ganglion cells. *Vision Res* **37**, 3483–3493.

Weiler R & Janssen-Bienhold U (1993). Spinule-type neurite outgrowth from horizontal cells during light adaptation in the carp retina: an actin-dependent process. *J Neurocytol* **22**, 129–139.